Original Article

Introduction of a Simple Algorithm to Create Synthetic-computed Tomography of the Head from Magnetic Resonance Imaging

Nahid Chegeni[1], Mohamad Javad Tahmasebi Birgani[2], Fariba Farhadi Birgani[1], Daryoush Fatehi[3], Gholamreza Akbarizadeh[4], Marziyeh Tahmasbi[5]

[1]Departments of Medical Physics and [2]Radiation Therapy and Medical Physics, Faculty of Medicine, Ahvaz Jundishapur University of Medical Sciences, Ahvaz, [3]Department of Medical Physics, Faculty of Medicine, Shakrekord University of Medical Science, Shakrekord, [4]Department of Electrical Engineering, Faculty of Engineering, Shahid Chamran University of Ahvaz, [5]Department of Radiologic Technology, Faculty of Para Medicine, Ahvaz Jundishapur University of Medical Sciences, Ahvaz, Iran

Abstract

Background: Recently, magnetic resonance imaging (MRI)-based radiotherapy has become a favorite science field for treatment planning purposes. In this study, a simple algorithm was introduced to create synthetic computed tomography (sCT) of the head from MRI. **Methods:** A simple atlas-based method was proposed to create sCT images based on the paired T1/T2-weighted MRI and bone/brain window CT. Dataset included 10 patients with glioblastoma multiforme and 10 patients with other brain tumors. To generate a sCT image, first each MR from dataset was registered to the target-MR, the resulting transformation was applied to the corresponding CT to create the set of deformed CTs. Then, deformed-CTs were fused to generate a single sCT image. The sCT images were compared with the real CT images using geometric measures (mean absolute error [MAE] and dice similarity coefficient of bone [DSC_{bone}]) and Hounsfield unit gamma-index (Γ_{HU}) with criteria 100 HU/2 mm. **Results:** The evaluations carried out by MAE, DSC_{bone}, and Γ_{HU} showed a good agreement between the synthetic and real CT images. The results represented the range of 78–93 HU and 0.80–0.89 for MAE and DSC_{bone}, respectively. The Γ_{HU} also showed that approximately 91%–93% of pixels fulfilled the criteria 100 HU/2 mm for brain tumors. **Conclusion:** This method showed that MR sequence (T1w or T2w) should be selected depending on the type of tumor. In addition, the brain window synthetic CTs are in better agreement with real CT relative to bone window sCT images.

Keywords: *Deformable registration, Demons algorithm, radiotherapy, synthetic computed tomography*

Introduction

Nowadays, magnetic resonance imaging (MRI) is increasingly employed in modern radiotherapy (RT) treatment planning systems (TPS) which improve target and organ at risk (OAR) definition in the brain and other sites as compared to CT-based delineations.[1,2] An accurate registration between MRI and CT images must be done to transfer the MRI delineations to the CTs. This is crucial to design a precise RT plan for cancer patients, especially for the head-and-neck treatment planning where sparing OAR is more critical.[3] The image registration in TPS introduces an error which results from the use of two-multimodality imaging (CT and MRI) and the time difference between the scans.[4-6] This error produces a systematic shift in the delineations which leads to target underdosage or the adjacent OARs overdosage.[7] Most recently, MRI-only based RT has been introduced which can eliminate the systematic registration errors with the use of a single-image modality.[8-10] In this approach, various methods apply to create synthetic CT (sCT) images using MR images; consequently CT images are not taken from the patients.[11] Using the sCT images have other advantages such as patient protection against ionizing radiation and reducing costs and clinical workload.[9]

Commonly, voxel-based, atlas-based, and hybrid methods are used to generate sCT images. In the voxel- based approach, a sCT image is generated from the individual voxel intensities in the MR scan.[12-14] The disadvantage of the some voxel-based methods is that, they need a specialized dual ultrashort echo time MRI sequence to make bone voxels separable from the air in the resulting MR images.[15-17] Another approach is atlas-based method, which estimates the sCT images using

How to cite this article: Chegeni N, Birgani MJ, Birgani FF, Fatehi D, Akbarizadeh G, Tahmasbi M. Introduction of a simple algorithm to create synthetic-Computed tomography of the head from magnetic resonance imaging. J Med Signals Sens 2019;9:123-9.

Received: June, 2018. **Accepted:** October, 2018.

Address for correspondence:
Dr. Fariba Farhadi Birgani, Department of Medical Physics, Ahvaz Jundishapur University of Medical Sciences, Ahvaz, Iran.
E-mail: farhadi.f92@gmail.com

Access this article online

Website: www.jmssjournal.net

DOI: 10.4103/jmss.JMSS_26_18

Quick Response Code:

conventional MRI sequences. In atlas-based method, first target-MR is registered with an atlas-MR then the obtained displacement fields are applied to CT-atlas and finally deformed-CTs are fused to create a single sCT image.[18-20]

In the atlas-based methods, despite the time-consuming and complexity of computation for creating of atlas database, the obtained sCT images suffer from registration errors and this is a serious matter.[21-23] To overcome these problems, we used a simple algorithm to create the atlas dataset and an intensity-based deformable algorithm (Demons) to register the target MR to atlas MR to decrease registration error. The reason for the use of the Demons algorithm is because studies on the extraction and classification of brain tumors for CT and MRI images showed that the features based on intensity are better.

Methods

In the proposed method, the steps for creating a sCT are as follows: (1) Collect a paired MRI and CT dataset, (2) Register each MR image from dataset to the target MR, (3) Apply the displacement field to the corresponding CT image from dataset, and (4) Fuse the collection of deformed CT images into a single sCT. The details of each step are describe in the following parts.

Image acquisition

In this study, 10 patients with Glioblastoma multiforme (GBM) and 10 patients with other brain tumors were selected from a collection of patients having previously undergone radiotherapy randomly. The MR images were acquired with a 1.5 T Siemens MAGNETOM Essenza including gradient echo T1-weighted (TR: 1900, TE: 5.1, FOV: 256 × 256, flip angle: 15) and T2-weighted (TR: 500, TE: 109, FOV: 256 × 256, flip angle: 15) with 1 mm × 1 mm × 1 mm voxel size and without contrast agent. In addition, the CT images which included brain and bone window, were collected with a Siemens SOMATOM Sensation 64 CT scanner (120 kv, 150 mAs and FOV: 256 × 256) with in-plane resolution of 0.5 mm × 0.5 mm and 1 mm slice thickness.

Creation paired magnetic resonance imaging and computed tomography dataset

To create paired MRI and CT dataset, it was necessary to carry out some preprocessing steps on CT and MR images. Gaussian filter was applied to eliminate the noise which acts as a destructive factor influencing the accuracy of registration. To separate the head from background, images were made binary, and then dilation and erosion morphological operations were applied by discs with a radius of 4 and 6 pixels, respectively. Ultimately, by multiplying to original image, the final image obtained without a background.

After preprocessing, CT and MR images were resampled and then CT-MR image pairs were registered using the Affine transformation model. This technique was applied to correct geometric distortions such as translation, scaling, similarity transformation, reflection, rotation, shear, and compositions of them. To register CT and MR images, the moving image (CT), the fixed image MRI and some parameters (optimizer, metric and iterations) were specified. The transformation matrix that maps points in moving image to corresponding points in fixed image was applied to the moving image to align it with the fixed image.

All of the above-mentioned processes were done by MATLAB 2015a software developed by MathWorks.

Generation synthetic computed tomography

To generate a sCT image, each MRI slices from dataset was registered to the target-MRI slices. The resulting transformations were applied to the corresponding CT from dataset for creating the set of deformed CT (CT_D) images. Then, CT_D images were fused to generate a single sCT [Figure 1].

An efficient nonparametric diffeomorphic image registration algorithm based on demons algorithm was used as presented by Vercauteren *et al*.[24] to register target-MR and MR form dataset. The Demons algorithm is a popular algorithm for nonrigid image registration because of its linear computational complexity and ease of implementation in MATLAB software. It approximately solves the large geometric differences problem by successively estimating force vectors that correspond to the vibrational derivative of the dissimilarity measure and smoothing.[24]

The Demons algorithm estimates the displacement field by aligning the target MR with the MR data set images. If the target-MR image size is $m \times n$, the output of the Demons is two matrices $m \times n$, in which the first matrix

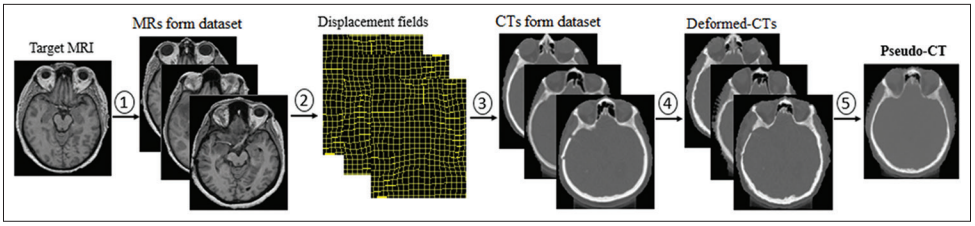

Figure 1: Steps of creating synthetic computed tomography: registering each magnetic resonance image form dataset to the target-magnetic resonance (1) calculating of displacement fields (2), applying the same transformation to the corresponding computed tomography form dataset (3), generating deformed CTs (4), and Fusing the collection of deformed CTs into a single synthetic computed tomography (5)

represents displacement values along x-axis and the second matrix represents displacement values along the y-axis. The displacement values are in pixel. The obtained displacement fields were applied to the corresponding CT from dataset images by the nearest-neighbor interpolation method and deformed CTs (CT_Ds) -were created. Finally, the CT_D images were fused to produce a single sCT in which the pixel value at each point of the sCT image was the median pixels of the deformed CT images at the corresponding point. The following algorithm was applied for fusion:

- (m, n) = size (CT_{Dl});
- i = 1:m
- j = 1:n
- sCT (i, j) =median (CT_{D1} [i, j], CT_{D2} [i, j],…, CT_{D9} [i, j]);

Where CT_{Dl} is the deformed CT image and the index of l is the patient's number.

Evaluation

To evaluate the generated sCT image, a comparison was made with the real CT using geometric measures and Hounsfield unit gamma-index.

Geometric measures

Probably the simplest and the most commonly criteria to evaluate syntactic CT is the geometric mean absolute error (MAE), defined as:

$$MAE = \frac{1}{N}\sum_{j=1}^{N}\left|HU_{CT}(j) - HU_{sCT}(j)\right| \quad (1)$$

Where N (=m × n) is the total number of pixels inside the body outline of the real CT and sCT images and HU represents Hounsfield unit values of the CT and sCT at corresponding pixel j^{th}. The Dice similarity coefficient (DSC) is a simple and useful measure to estimate spatial overlap which can be applied to study of reproducibility and accuracy in the created sCT images. DSC is defined for bone as:

$$DSC_{bone} = \frac{2\left(V_{bone}^{sCT} \cap V_{bone}^{CT}\right)}{\left(V_{bone}^{sCT} \cup V_{bone}^{CT}\right)} \quad (2)$$

Where V_{bone}^{sCT} and V_{bone}^{CT} are volumetric bone structures in binary image for the sCT and the real CT images, respectively. DSC will result in a value between 0 and 1, which implies no and complete overlap, respectively.

Hounsfield unit Gamma Index (Γ_{HU})

CT and consequently sCT images are of low resolution and less sensitive to spatial differences. Therefore; we applied an error measure as γ-index for HU which first proposed by Sjölund *et al*.[18] They adapted the conventional gamma-index, used for dose distribution comparison, to determine the HU deviation (ΔH = 100 HU) for all pixels. Accordingly, Γ_{HU} (i, k) for pixel (i, k) is calculated as:

$$\Gamma_{HU}(i,\mathrm{k}) = min_{\substack{v=1 \text{ to } m \\ w=1 \text{ to } n}}\left(\sqrt{\left(\frac{HU_{sCT}(i,k) - HU_{CT}(v,w)}{\Delta H}\right)^2 + \left(\frac{x(i,k) - x(v,w)}{\Delta x}\right)^2}\right) \quad (3)$$

Where HU_{sCT} (i, k) and HU_{CT} (v, w) are the Hounsfield units at coordinate x (i, k) and x (v, w), respectively. All calculations were done using MATLAB 2015a.

Results

The sCT images were generated based on T1 and T2 weighted in two modes of bone and brain window. For a particular slice of the patient tomographic images [Figure 2], bone outline in the real CT and sCT images and real and sCT slices subtraction were displayed. As can be seen visually, the bone outline in sCT based on T1-weighted MRI is more accommodate to real-CT, which may be due to the higher bone signal strength of T1 compared to T2 sequence [Figure 2b]. The subtraction of the corresponding CT and sCT represents the more difference between brain window real CT and sCT [Figure 2c]. This is probably because of the greater contrast of the soft tissues in MR than CT images.

A comparison of sCTs with the real CT images were done using geometric measures (MAE and DSC of bone [DSC_{bone}]) and Γ_{HU} with criteria 100 HU/2 mm summarized in Table 1. The HU gamma analysis in Table 1 includes the average of the Γ_{HU} and the percentage of the pixels with Γ_{HU} greater than 1 (e.g., mismatch percentage).

To evaluate further the validity of this method in GBM samples, tumor area was extracted in two groups CT and sCT and then MAE and Γ_{HU} were compared. The average MAE and Γ_{HU} were obtained as 18 ± 5.2 HU and 0.11 ± 0.08 for brain window sCTs based on T1 and 14 ± 2.1 HU and 0.09 ± 0.03 sCTs based on T2, respectively (not included here). As expected, this assessment gives results similar to Table 1.

Discussion

In this study, a simple and fast method was introduced to create sCT from MR images using atlas-based method. We used the general software (MATLAB) which is simple and relatively fast approach. For example, to create a sCT, it takes about 3 min on a Core i5 PC system which is less than the time reported by atlas-based studies which takes about 25, 16, and 38 min.[11,19,25] In this study to create MR-CT pairs, the simple processes were performed such as noise filtration, background separation, image resampling, and registration while the atlas data set is produced by complex and time-consuming algorithms.[20] In addition, an efficient nonparametric diffeomorphic image registration algorithm-based Demons algorithm was used which has lower target registration error than the original Demons algorithm.[24]

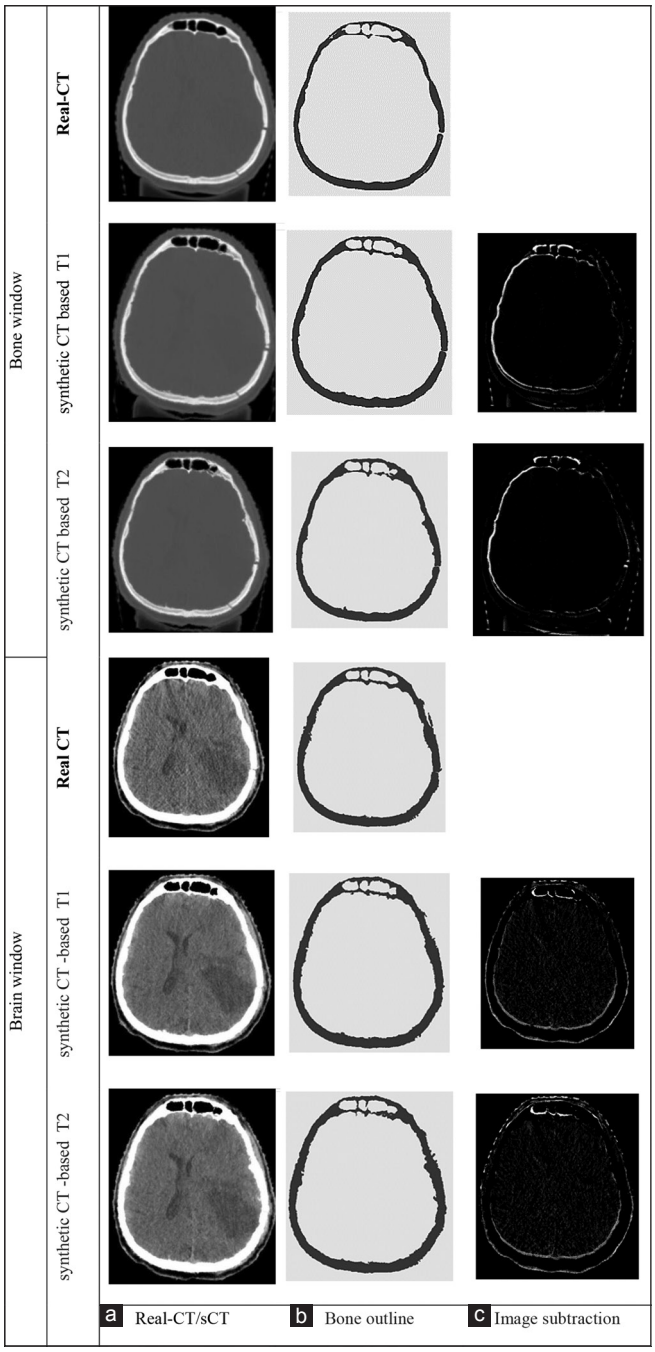

Figure 2: (a) Axial slices for bone and brain window synthetic computed tomography based on T1 or T2 weighted and real computed tomography. (b) Bone outline. (c) The subtraction of the corresponding Real CT and synthetic CT

The distinction between our method and Atlas-based method was explained using T1 or T2-weighted images in the brain region while the corresponding method often employed just T1-weighted as MR target.[26] According to Table. 1 for brain tumors except GBM, the best results (minimum MAE and maximum DSC_{bone}) occurred when using T1-weighted MRI data set. For GBM samples, the sCTs generated by T2-weighted showed better results in both the bone and brain widow than T1 target. This may be related to the ability of the T2-weighted images to display GBM and it is usually accompanied with edema that has a stronger signal in a T2 sequence. In general, T1-based sCTs represent a greater bone DSC due to the stronger bone signal with respect to T2 for all samples.

Table 1: The average value and standard deviation of the mean absolute error, Dice similarity coefficient of bone, Hounsfield Unit gamma-index and percentage of pixels with Hounsfield Unit gamma-index >1 are shown for 10 patients with glioblastoma multiforme and 10 patient with other brain tumor

Synthetic CT	$\overline{MAE}$ (HU)	$\overline{DSC}_{bone}$	$\overline{\Gamma}_{HU}$	$\%\Gamma_{HU} > 1$ *
For GBM				
T1-based (bone window)	85±14.7	0.85±0.06	0.52±0.33	17±8
T2-based (bone window)	83±15.3	0.80±0.02	0.44±0.2	15±4
T1-based (brain window)	80±10.8	0.83±0.05	0.37±0.21	10±6
T2-based (brain window)	78±8.1	0.82±0.02	0.29±0.16	7±2
For other brain tumors				
T1-based (bone window)	83±12.4	0.89±0.03	0.59±0.19	13±7
T2-based (bone window)	93±13	0.82±0.01	0.64±0.32	19±8
T1-based (brain window)	80±9.7	0.85±0.04	0.36±0.18	9±1.3
T2-based (brain window)	82±8.3	0.84±0.02	0.38±0.21	11±5

*Percentage of pixels with Γ_{HU} >1. CT – Computed tomography; GBM – Glioblastoma multiforme; MAE – Mean absolute error; DSC_{bone} – Dice similarity coefficient of bone; HU – Hounsfield unit; Γ_{HU} – HU gamma-index

For all brain tumors except GBM, minimum Γ_{HU} occurred for the brain window sCTs based on T1-weighted MR imaging and only 9% ± 1.3% of the pixels did not pass gamma criteria. While in GBM samples, the average of Γ_{HU} and the percentage of the pixels with Γ_{HU} larger than 1 dropped to 0.29% ± 0.16% and 7% ± 2%, respectively, which is related to brain window sCTs based on T2-weighted.

By reviewing previous studies on atlas-based methods, the range of the MAE and DSC_{bone} for brain was displayed between 97 and 114 HU and 0.63–0.83, respectively.[18,19,24,25,27-29] The average MAEs for the multimodal methods showed 118.7 ± 10.4 HU for the voxel-based and 73.0 ± 6.4 HU for the patch-based algorithm[30] and 99.69 ± 11.07 HU for the multiscale and dual-contrast patch-based method using a MR target.[31] The feasibility of using from T1w and T2w as target for generating sCT in the brain was investigated that Mean absolute error for the sCT was 124 ± 10 HU.[32] Our

results also included 78–93 HU and 0.80–0.89 for MAE and DSC_{bone} respectively, which is in agreement with the results of previous studies. Probably the higher precision of the produced synthetic-CTs in this study than the other methods of deformable atlas based methods is due to the high efficiency of algorithms based on intensity such as demons.

From Table 1, the maximum DSC bone is related to bone window sCT based on T1 in all samples. This is probably due to the capability of the T1-weighted images in transferring bone geometry more efficient than T2 weighted.

In addition to quantities MAE and DSC_{bone}, Γ_{HU} was used which is particularly suitable for high-contrast objects with small displacements.[18] For GBM, Γ_{HU} showed smaller amount for T2-based sCT. Therefore, it may be better to test all image types (T1/T2 and brain/bone window CT) for any kinds of brain tumors, separately. The results of Γ_{HU} are in good agreement with the MAE [Table 1], and in other words, confirm each other. For example, in cases where MAE is the maximum, Γ_{HU} is high and vice versa.

For future studies, we suggest to apply all MR image sequences such as T1w/T2w and brain/bone window CT to create a dataset for other tumors.

Conclusions

This study introduced a simple and fast method to generate sCT images using atlas-based approach, which it could potentially be useful for the MR-guided radiotherapy TPS. This study concluded that MR sequence (T1w or T2w) should be selected according to the tumor type for better s CT accuracy.

Financial support and sponsorship

None.

Conflicts of interest

There are no conflicts of interest.

References

1. Prabhakar R, Haresh KP, Ganesh T, Joshi RC, Julka PK, Rath GK, *et al.* Comparison of computed tomography and magnetic resonance based target volume in brain tumors. J Cancer Res Ther 2007;3:121-3.
2. Rasch C, Steenbakkers R, van Herk M. Target definition in prostate, head, and neck. Semin Radiat Oncol 2005;15:136-45.
3. Roy S, Carass A, Jog A, Prince JL, Lee J, editors. MR to CT registration of brains using image synthesis. Proceedings of SPIE. International Society for Optical Enginering; 2014.
4. Cattaneo GM, Reni M, Rizzo G, Castellone P, Ceresoli GL, Cozzarini C, *et al.* Target delineation in post-operative radiotherapy of brain gliomas: Interobserver variability and impact of image registration of MR(pre-operative) images on treatment planning CT scans. Radiother Oncol 2005;75:217-23.
5. Ulin K, Urie MM, Cherlow JM. Results of a multi-institutional benchmark test for cranial CT/MR image registration. Int J Radiat Oncol Biol Phys 2010;77:1584-9.
6. Zitova B, Flusser J. Image registration methods: A survey. Image Vis Comput 2003;21:977-1000.
7. Nyholm T, Nyberg M, Karlsson MG, Karlsson M. Systematisation of spatial uncertainties for comparison between a MR and a CT-based radiotherapy workflow for prostate treatments. Radiat Oncol 2009;4:54.
8. Dowling JA, Lambert J, Parker J, Salvado O, Fripp J, Capp A, *et al.* An atlas-based electron density mapping method for magnetic resonance imaging (MRI)-alone treatment planning and adaptive MRI-based prostate radiation therapy. Int J Radiat Oncol Biol Phys 2012;83:e5-11.
9. Lee YK, Bollet M, Charles-Edwards G, Flower MA, Leach MO, McNair H, *et al.* Radiotherapy treatment planning of prostate cancer using magnetic resonance imaging alone. Radiother Oncol 2003;66:203-16.
10. Koivula L, Kapanen M, Seppälä T, Collan J, Dowling JA, Greer PB, *et al.* Intensity-based dual model method for generation of synthetic CT images from standard T2-weighted MR images – Generalized technique for four different MR scanners. Radiother Oncol 2017;125:411-9.
11. Chen S, Quan H, Qin A, Yee S, Yan D. MR image-based synthetic CT for IMRT prostate treatment planning and CBCT image-guided localization. J Appl Clin Med Phys 2016;17:236-45.
12. Berker Y, Franke J, Salomon A, Palmowski M, Donker HC, Temur Y, *et al.* MRI-based attenuation correction for hybrid PET/MRI systems: A 4-class tissue segmentation technique using a combined ultrashort-echo-time/dixon MRI sequence. J Nucl Med 2012;53:796-804.
13. Edmund JM, Kjer HM, Van Leemput K, Hansen RH, Andersen JA, Andreasen D, *et al.* A voxel-based investigation for MRI-only radiotherapy of the brain using ultra short echo times. Phys Med Biol 2014;59:7501-19.
14. Rank CM, Hünemohr N, Nagel AM, Röthke MC, Jäkel O, Greilich S, *et al.* MRI-based simulation of treatment plans for ion radiotherapy in the brain region. Radiother Oncol 2013;109:414-8.
15. Johansson A, Karlsson M, Nyholm T. CT substitute derived from MRI sequences with ultrashort echo time. Med Phys 2011;38:2708-14.
16. Johansson A, Karlsson M, Yu J, Asklund T, Nyholm T. Voxel-wise uncertainty in CT substitute derived from MRI. Med Phys 2012;39:3283-90.
17. Keereman V, Fierens Y, Broux T, De Deene Y, Lonneux M, Vandenberghe S, *et al.* MRI-based attenuation correction for PET/MRI using ultrashort echo time sequences. J Nucl Med 2010;51:812-8.
18. Sjölund J, Forsberg D, Andersson M, Knutsson H. Generating patient specific pseudo-CT of the head from MR using atlas-based regression. Phys Med Biol 2015;60:825-39.
19. Uh J, Merchant TE, Li Y, Li X, Hua C. MRI-based treatment planning with pseudo CT generated through atlas registration. Med Phys 2014;41:051711.
20. Toga AW, Thompson PM. The role of image registration in brain mapping. Image Vis Comput 2001;19:3-24.
21. Han X. MR-based synthetic CT generation using a deep convolutional neural network method. Med Phys 2017;44:1408-19.
22. Ghose S, Dowling JA, Rai R, Liney GP. Substitute CT generation from a single ultra short time echo MRI sequence: Preliminary study. Phys Med Biol 2017;62:2950-60.
23. Ghose S, Greer PB, Sun J, Pichler P, Rivest-Henault D,

Mitra J, *et al.* Regression and statistical shape model based substitute CT generation for MRI alone external beam radiation therapy from standard clinical MRI sequences. Phys Med Biol 2017;62:8566-80.

24. Vercauteren T, Pennec X, Perchant A, Ayache N. Diffeomorphic demons: Efficient non-parametric image registration. Neuroimage 2009;45:S61-72.
25. Andreasen D, Van Leemput K, Hansen RH, Andersen JA, Edmund JM. Patch-based generation of a pseudo CT from conventional MRI sequences for MRI-only radiotherapy of the brain. Med Phys 2015;42:1596-605.
26. Edmund JM, Nyholm T. A review of substitute CT generation for MRI-only radiation therapy. Radiat Oncol 2017;12:28.
27. Stanescu T, Jans HS, Pervez N, Stavrev P, Fallone BG. A study on the magnetic resonance imaging (MRI)-based radiation treatment planning of intracranial lesions. Phys Med Biol 2008;53:3579-93.
28. Schreibmann E, Nye JA, Schuster DM, Martin DR, Votaw J, Fox T, *et al.* MR-based attenuation correction for hybrid PET-MR brain imaging systems using deformable image registration. Med Phys 2010;37:2101-9.
29. Kops ER, Hautzel H, Herzog H, Antoch G, Shah NJ. Comparison of template-based versus CT-based attenuation correction for hybrid MR/PET scanners. IEEE Trans Nucl Sci 2015;62:2115-21.
30. Speier C, Pileggi G, Izquierdo-Garcia D, Catana C, Sharp GC, Spadea MF, *et al.* Advanced multimodal methods for cranial pseudo-CT generation validated by IMRT and VMAT radiation therapy plans. Int J Radiat Oncol Biol Phys 2018;102:792-800.
31. Aouadi S, Vasic A, Paloor S, Torfeh T, McGarry M, Petric P, *et al.* Generation of synthetic CT using multi-scale and dual-contrast patches for brain MRI-only external beam radiotherapy. Phys Med 2017;42:174-84.
32. Pileggi G, Speier C, Sharp GC, Izquierdo Garcia D, Catana C, Pursley J, *et al.* Proton range shift analysis on brain pseudo-CT generated from T1 and T2 MR. Acta Oncol 2018;57:1521-31.

BIOGRAPHIES

Nahid Chegeni received the master's degree in Medical Physics in 2002 from Iran Medical Science University, Tehran and PhD degree in Medical Physics in 2013 from Ahvaz Jundishapur University of Medical Sciences. She is an assictant professor at Department of Medical physics in Ahvaz Jundishapur University of Medical Sciences. Her research interests are radiotherapy, dosimetry, Monte Carlo simulation, and imaging in radiotherapy.

Email: chegenin@gmail.com

Mohammad Javad Tahmasebi Birgani received the master and Ph.D degree in Nuclear Physics in 1987 and 1992 from Shiraz university, respectively. He is an professor at Department of Radiation therapy and Oncology Ahvaz Jundishapur University of Medical Sciences. His research interests are radiotherapy, dosimetry, and imaging in radiotherapy.

Email: tahmasebi_mj@yahoo.com

Fariba Farhadi Birgani is the PhD student of Medical Physics at the Jundishapur University of Medical Sciences, Ahvaz, Iran. She received her MSc degree in in Medical Physics in 2014 from Ahvaz Jundishapur University of Medical Sciences. Iran. Her research interests include radiotherapy, medical imaging, image processing, machine vision, and machine learning.

Email: farhadi.f92@gmail.com

Daryoush Fatehi obtained his B.Sc., in Diagnostic Radiology Technology, from the Mashhad University of Medical Sciences, Mashhad, Iran in December 1993. He studied Medical Physics at the Tarbiat Modarres University, Tehran, Iran; where he graduated as a M.Sc. in December 1996. To perform his Ph.D. project, he joined the Hyperthermia Unit, department of Radiation Oncology, at the Erasmus University in Rotterdam, the Netherlands in October 2003. His research interests are hyperthermic oncology and medical imaging.

Email: d.fatehi@gmail.com

Gholamreza Akbarizadeh received the B.S. degree from the Khajeh-Nassir Tousi University of Technology (KNTU), Tehran, Iran, in 2003 and the M.S. and Ph.D. degrees from the Iran University of Science and Technology, Tehran, Iran, in 2005 and 2011, respectively, all in electrical and electronics engineering. From 2003 to 2011, he has worked at the DSP R&D research laboratory as a senior researcher. He is currently an Assistant Professor and Faculty Member of the Electrical Engineering Department at Shahid Chamran University of Ahvaz (SCU), Ahvaz, Iran. His research interests include machine vision, image processing, remote sensing analysis, and geographic information system (GIS) techniques for earth surface mapping.

Email: gholamrezaakbari@gmail.com

Marziyeh Tahmasbi obtained her BSc. in Biomedical Engineering from Ahvaz Jundishapur University of Medical Sciences in 2002 and her MSc in Biomedical Engineering from Shahid Beheshti University of Medical Sciences in 2009. She has received her Medical Physics PhD degree from Ahvaz Jundishapur University of Medical Sciences, in 2017. She is an Assistant professor at Department of Radiologic Technology Ahvaz Jundishapur University of Medical Sciences. Her research interests include medical imaging, Image processing, Radiation therapy and Radiation protection.

Email: tahmasbi-m@ajums.ac.ir